# FLOW OF DRAG REDUCING FLUIDS THROUGH A SUDDEN ENLARGEMENT

*M.H.Embaby and M.A. El-Kady*

Mechanical Power Engineering Department, Faculty of Engineering, Minufiya University,Egypt.

*Abstract*

Theoretical and experimental studies, of drag reducing dilute polymer solution flow through a sudden enlargement, are carried out. A turbulence model, which has been early used for predicting Newtonian flows with adverse pressure gradient (APG), is developed in the present analysis. The developed model well predicts the fully developed drag reduction flow in pipes, i.e. flow under favorite pressure gradient (FPG) conditions besides the sudden enlargement (APG) flow. Predictions, of the mean flow properties and turbulence characteristics of drag reduction turbulent flows in a sudden enlargement -i.e. under (APG)- are obtained and discussed. An experimental setup is established for studying the pressure characteristics of the flow through a (2:1) diameter ratio sudden enlargement test section. The working fluids are dilute solutions of Polyethylene Glycol (PEG) polymer in tap water. Comparison between theoretical and experimental pressure distribution results shows a reasonable agreement. It is concluded that the developed turbulence model can be used to predict drag reducing polymer flows under both (FPG) and (APG) conditions.

## *1. Introduction*

Sudden enlargement flows find wide applications in hydraulic circuits while drag reducing fluids have been considered extensively in recent researches. The flow through a sudden enlargement is an adverse pressure gradient (APG) one. Review of previous related work on both Newtonian and drag reducing fluid turbulent flows under favorite pressure gradient (FPG) or (APG) may help in understanding the problem.

Turbulent Newtonian flows under (FPG) have been widely studied and predictions of such flows using turbulence models are extensive [1,2,3,4]. The 'k- ε' model has been the most familiar one used for simulating such flows. A wide discussion of this model has been presented in many sources as, for example, the work due to Jones and Launder [2].

---

***Manuscript received from Dr. M.A. El-Kady on : 24/11/1999***
***Accepted on : 14/12/1999***
***Engineering Research Bulletin, Vol 23,No 1, 2000 Minufiya University, Faculty of Engineering , Shebien El-Kom , Egypt, ISSN 1110-1180***

Turbulent Newtonian flow through a sudden enlargement had been simply analyzed and presented in many texts [5,6] where expressions for both pressure recovery and loss coefficient could be obtained using experimental closures. Predictions of the mean flow properties for turbulent separated flows, using integral methods, have been carried out by some authors [7]. Predictions of Newtonian (APG) flows using turbulence models seem to be little. For example, Khalifa et al. [8] used the conventional ' k-ε ' model to predict turbulent Newtonian flows in highly curved ducts and their predictions indicated an (APG) at the inner wall. Recently Hattori and Nagano [9] introduced a 'k-ε' model which takes into account the effect of pressure gradient and successfully simulates both (FPG) and (APG) flows. Their predictions were compared with experimental and direct simulation data and a good agreement over a wide range of pressure gradient was indicated.

Turbulent drag reducing fluid flows, under (FPG), have been studied by many authors. Wide studies [10, 11] have been concerned with drag reducing polymer solution flows through a straight pipe. Virk [ 11 ] had defined the phenomenon of drag reduction and discussed widely both the mean and turbulent characteristics of such flows. Also, he gave empirical expressions for the eddy viscosity profiles during drag reduction. Predictions of turbulent drag reduction flows under (FPG), by developing turbulence models, have been carried out by many authors [12,13,14,15,16]. These models are based on the Newtonian flow models. For example, Rogeri [14], suggested inclusion of the double and triple turbulence correlation in the Newtonian one dimensional shear flow equations. Then, he introduced the viscoelastic effects –i.e. polymeric parameters- into the governing equations and predictions of the onset conditions in addition to the percentage drag reduction could be achieved. Durst and Rastogi [15], introduced a damping factor to an earlier Newtonian turbulence model. The parameters of this factor are dependent on polymer, solvent and the fully developed mean velocity profiles. Predictions of the mean flow and turbulence properties were reasonably confirmed experimentally. Recently, Idir and Siamack [16] used a one-layer turbulent eddy viscosity model for predicting drag reduction flow through annular pipe. The model is based on the mixing length approach wherein a damping factor is used in order to account for the near wall effects. Drag reduction effects are, then, simulated with a variable damping parameter in the eddy- viscosity expression. A procedure for determining the value of that parameter from the fully developed pipe flow friction data was discussed. Comparison between predicted and measured mean flow and turbulence quantities indicated a reasonable agreement.

Turbulent drag reducing fluid flows under (APG) have received little attention.. The available studies for such flows have been restricted to experimental ones. For example, Kato and Shibanuma[17], studied experimentally the flow of dilute polymer solutions through diverging and converging cross sections. They showed that in a converging flow, no remarkable drag reduction was observed. On the other hand, in a diverging flow through a - five degree angle- diffuser they observed a pressure recovery which was about 30% larger than Newtonian flow at a certain polymer concentration. Tachibana and Kita [18] studied experimentally drag reducing polymer turbulent flow through (1.76:1) and (2.6:1) diameter ratio sudden enlargement sections. They showed that the polymer affects considerably the loss coefficient, the pressure recovery and drag reduction appearance in both the upstream and downstream parts of the sudden enlargement.

The above review shows that predictions of turbulent drag reduction flows under (APG) still need more investigation. Therefore, the objective of the present work is to develop a ' k-ε ' model for such flows and to predict drag reducing fluid turbulent flow in a sudden enlargement using this model.

## 2. *Analysis*

The procedures followed earlier for developing turbulence models of turbulent drag reduction flows under (FPG) are adapted in the present work. Thus, the model suggested early by Hattori and Nagano [9], for turbulent Newtonian flows under (APG) , is developed to simulate drag reduction flows under (APG) . This is carried out by introducing a damping factor ( Df) which simulates the drag reduction effects.

### *2.1 The governing equations and boundary conditions*

The governing conservation equations; for steady two dimensional turbulent flow of an incompressible fluid through a pipe; involve the continuity, momentum in addition to the turbulence " k-ε " model- namely the turbulent kinetic energy 'k' and its dissipation rate' ε ' - equations[19]. These equations are rearranged and a set of differential equations, for the fluxes of the different flow properties, can be written in a general form [20]. The dimensionless general form of these equations, in the cylindrical (x, r) coordinate system, is written as:

$$\frac{\partial[ur\phi-\Gamma_\phi r\frac{\partial\phi}{\partial x}]}{\partial x}+\frac{\partial[vr\phi-\Gamma_\phi r\frac{\partial\phi}{\partial r}]}{\partial r}=S_\phi \qquad (1)$$

, where x = x'/D' and r = r'/D' are the dimensionless coordinates while D' is the pipe diameter. The parameter $\phi$ can stand for any dimensionless transport property such as the axial velocity component (u = u'/U' ), the radial component (v = v'/U') ,the turbulent kinetic energy (k =k'/ U'$^2$ ) or its dissipation rate (ε = ε $\rho$ D'/U' ), where U' is the average flow velocity in the pipe. The parameter ($\Gamma_\phi$ = $\Gamma_\phi$' / $\rho$ U'D' ) stands for the corresponding dimensionless diffusion coefficient while $S_\phi$ stands for the corresponding dimensionless source term . Table (1) includes those parameters for the different conservation equations.

TABLE (1): Diffusion Coefficients and Source Terms.

| conservation of | $\phi$ | $\Gamma_\phi$ | $S_\phi$ |
|---|---|---|---|
| mass | 1 | 0 | 0 |
| axial momentum | $u$ | $\mu_e$ | $-r\frac{\partial p}{\partial x}+\frac{\partial(\mu_e r\frac{\partial u}{\partial x})}{\partial x}+\frac{\partial(\mu_e r\frac{\partial v}{\partial x})}{\partial r}-\frac{2}{3}\frac{\partial rk}{\partial x}$ |
| radial momentum | v | $\mu_e$ | $-r\frac{\partial p}{\partial r}+\frac{\partial(\mu_e r\frac{\partial u}{\partial r})}{\partial x}+\frac{\partial(\mu_e r\frac{\partial v}{\partial r})}{\partial r}-\frac{2}{3}r\frac{\partial k}{\partial r}-2\mu_e\frac{v}{r}$ |
| turbulent kinetic energy | k | $\frac{\mu_e}{\sigma_k}$ | $rP_k-r\varepsilon$ |
| turbulent kinetic energy dissipation rate | $\varepsilon$ | $\frac{\mu_e}{\sigma_\varepsilon}$ | $C_1 r\frac{\varepsilon}{k}P_k-C_2 f_\varepsilon r\frac{\varepsilon^2}{k}$ |

$$P_k = \mu_e[2((\frac{\partial u}{\partial x})^2 + (\frac{\partial v}{\partial r})^2 + (\frac{v}{r})^2) + (\frac{\partial v}{\partial x} + \frac{\partial u}{\partial r})^2] \quad (2)$$

, $\mu_e$ is the dimensionless effective viscosity, given by:

$$\mu_e = \mu_t + \mu_l \quad (3)$$

, $\mu_l$ is the dimensionless molecular viscosity while $\mu_t$ is eddy viscosity given by:

$$\mu_t = C_\mu f_\mu k^2/\varepsilon \quad (4)$$

The model constants and functions are shown in Table ( 2 ) below.

TABLE (2): Model Constants and Functions

| $C_\mu$ | $C_1$ | $C_2$ | $\sigma_k$ | $\sigma_\varepsilon$ | $f_\mu$ | $B_1$ | $B_2$ |
|---|---|---|---|---|---|---|---|
| .09 | 1.45 | 1.9 | 1.4 | 1.3 | $[1-\exp(-y^+/A^+)]^2$ * $\{1+(B_1/R_t^{3/4})\exp[-(R_t/B_2)^2]\}$ | 20 | 120 |

| $A^+$ | $f_\varepsilon$ |
|---|---|
| $Df/(1+11.8P^+)$ | $1-.3\exp(-R_t^2)$ |

where $R_t$ is the turbulence Reynolds number, $R_t = k^2/\nu\varepsilon$.

The parameter $A^+$, which organizes from Van Driest constant, is a function of the pressure gradient term $P^+$ as shown in the table. For Newtonian flows , the numerator of this function was assigned a constant value of 30 [9] on the basis of direct numerical simulation(DNS) data of the near wall regions of such flows. In the present model the numerator 'Df ' is allowed to vary in order to simulate the drag reduction effects. It is seen from table (2) that the function $f_\mu$, and consequently the eddy viscosity $\mu_t$ [eq.(4)] , decrease as 'Df ' increases. Thus, the factor 'Df 'is used as a damping factor in the present prediction scheme. Also, as drag reduction is essentially a near wall phenomenon [11,13], these expressions are used for $y^+ < 150$. In the turbulent core region, i.e. $y^+ > 150$, the parameter $f_\mu$ is set to unity. The pressure gradient term $P^+$ is evaluated at the pipe centerline in the prediction scheme.

The governing equations (1) are solved numerically by means of Patankar's [20] finite volume technique. Figure (1) shows the geometry and calculation domain. A 20x20 non-uniform grid point network is used. In x-direction the step length (dx) is given by: $(dx)_{i+1} = 1.2*(dx)_i$. In the r- direction, the 1st five steps are decreasing as the wall is approached having the values: dr= 0.002,0.004,0.008,0.016 and 0.032. The remaining, core steps are uniform and have the value of 0.0324. This allowed avoiding the near wall approximations since the wall law constants for drag reducing flows differ from the Newtonian flow ones. A staggered grid is adapted such that the scalar variables (p, k, ε) are stored at nodal points while the velocities (u, v) are stored at points midway between the nodal points in x and r directions respectively. The governing differential eqs.(1) are integrated over the appropriate control cell(dx..dr)

using a power law scheme for the property distribution between the appropriate grid points. The resulting, finite difference, equations are solved by iteration using the 'SIMPLE' algorithm [20]. Iteration is carried out, line-by-line in x direction, and the dimensionless mass flow rates and residuals of the different variables are calculated all over the domain lines. Iteration is stopped when the largest of them becomes less than a convergence criterion of $10^{-2}$- $10^{-4}$. A maximum deviation of $\pm$ 2% of the predicted properties is noticed for the above range of convergence criterion. Also, suitable relaxation factors are used in order to control convergence and execution time. Low relaxation factors- as low as '.2'- are used in case of high Reynolds numbers and/or large diameter ratio of sudden enlargement. The domain lengths are X=25 and R=0.5 in x and r directions respectively. Predictions are obtained for axial lengths which are multiple of 25 where the initial conditions for a current domain are set equal to the output of the preceding domain. This allowed obtaining a fully developed pipe flow predictions in both of the upstream and down stream pipes of the sudden enlargement.

The boundary conditions are specified as follows:

i) $u = v = k = \varepsilon = 0$ at the walls while at symmetry axis : $\partial / \partial x = 0$.

ii) at entrance to the first domain of the upstream pipe a uniform profiles are assumed thus: u=1, v= k= ε= 0.0

iii) at the side wall of the sudden enlargement a wall function treatment is adopted to reduce the required grid points in the axial direction. Thus, the near wall radial velocity $v_w$ ,at the nearest grid point , is assumed to be given by :

$$\frac{v_w}{u_{tr}} = 2.5 \ln x^+_w + 5.5 \qquad (5)$$

where $u_{tr}$ *and* $x_w^+$ are the dimensionless side wall shear velocity and grid point distance respectively, given by:

$$u_{tr} = \sqrt{\tau_{wr}} \qquad \textit{and} \quad x_w^+ = \frac{x_w u_{tr}}{v} \qquad (6)$$

In pipe flow predictions, the predicted dimensionless parameters are normalized using the pipe diameter and average velocity (D' and U') as discussed above. On the other hand, in sudden enlargement predictions, the downstream dimensionless parameters are normalized using the upstream ($D_1'$ and $U_1'$) parameters for the aim of comparison. Before predicting drag reduction flows, the model is tested to provide confidence in its performance in some previously well known flows. For example, Figs.(2 ) and (3) show predictions of the fully developed velocity profiles and the friction factor relationships at a damping factor Df=20 compared to the well-known early Newtonian correlation [11].

### *2.2. Predictions of fully developed drag reduction flows in pipes*

Drag reduction flows are simulated by varying the damping factor 'Df ' in the turbulence model. This is clearly depicted from the conventional 'u+-y+' or ' f-Re' predicted plots shown in Figs. (2) and (3) respectively. The well- known Newtonian correlation and Virk's maximum drag reduction (mdr) asymptote [11] are represented in the figures for comparison. It is seen that the model simulates well the drag reduction effects and that the two extreme cases of Newtonian and maximum drag reduction (mdr) flows are predicted at Df=20 and 70 respectively. The polymeric flow regimes [11] are predicted at 20<Df<70. It is seen, from Fig.(2), that an elastic sub-layer defined earlier by Virk, i.e. a layer having a velocity profile described by the

(mdr) asymptote; exists. The thickness of that layer is polymer- solvent system dependent and the (mdr) flow conditions are attained as that layer fills the whole pipe cross section. Durst and Rastogi[12 ], proposed a sophisticated and approximate procedure in order to determine the damping factor- in their model- from the 'u+-y+ ' data of the polymer solution. However, a simple procedure is proposed in the present work for determining the damping factor' Df ' from the polymer solution 'f-Re' data. Thus, for a certain polymer solution the fully developed flow friction data are allocated on Fig.(3) and then the corresponding damping factor 'Df" is determined.
It is worthy to note that roughness affect drag reduction [21] by reducing the elastic sub-layer thickness and hence increasing the friction factor under the same flow rates or Reynolds numbers. This means, simply, that flows through rough pipes are predicted at less 'Df ' values. Thus the above suggested procedure of prediction can be applied on rough pipes also. Accordingly, Newtonian flows through rough pipes are predicted at Df< 20 while the (mdr) flows are predicted at Df<70.

### *2.3 Predictions of drag reduction flow in a sudden enlargement*

Predictions of sudden enlargement flow are obtained using different 'Df ' values at the upstream pipe and the results of the mean flow and turbulence characteristics at the downstream pipe are shown in Figs.(4) through (10). In addition to the mean flow velocity and pressure distributions, the following parameters are evaluated.

i) the pressure recovery coefficient Cp, defined as:

$$Cp=P_{w,max} \qquad (7)$$

ii) the rate of pressure recovery G, defined as[20]:

$$G=(P_{w,max}-P_w)/P_{w,max} \qquad (8)$$

iii) the pressure recovery distance Xp at which the pressure attains its maximum value Cp.

iv) the sudden enlargement loss coefficient $\xi$, defined from:

$$\xi = 2\,\Delta P_l \qquad (9)$$

where $\Delta P_l$ is the loss in the theoretical pressure recovery , calculated as:

$$\Delta P_l = 1-AR^2 - Cp \qquad (10)$$

### *Results and discussion*

Samples of the results are shown in Figs.(4) through (10 ). The same trends prevail for other parameters affecting the flow such as the diameter ratio and the flow Reynolds number. Therefore, the discussion will emphasize the drag reduction effects.

### *Pressure distribution*

Samples of the wall static pressure distributions for a (1.75:1) diameter ratio sudden enlargement are shown in Fig.(4 ). These distributions are for the two extreme values of the damping factor 'Df', namely Df=20 (Newtonian) and Df=70 (mdr), at two different Reynolds numbers. Figure(4.a) shows that, for downstream distances x<5 and at low Reynolds number, the rate of pressure recovery under (mdr) conditions is lower than that under Newtonian flow conditions. This is attributed to the lower radial momentum transfer in the wall region under (mdr) flow conditions. On the other

hand, Fig.(4) shows that for downstream distances x>5 the distributions have the same trends while the pressure at any section under (mdr) conditions is higher than that under the Newtonian ones. It is also seen that drag reduction effects decrease as Reynolds number increases. This means that at high Reynolds numbers the loss in pressure is mainly determined by secondary flow rather than by wall friction effects. The results of pressure distribution parameters such as the maximum pressure recovery 'Cp', the loss coefficient ' $\xi$ ' and the pressure recovery length 'Xp' are shown in Figs.(5) through (8).The figures show that as drag reduction, i.e. Df, increases both of ' Cp' and' Xp' increase while '$\xi$' decreases.
Figures(5) and(6) can be used for design purposes where plots of 'Cp' for different 'Df', 'Re' and diameter ratio'D2/D1' values are presented. It is observed that drag reduction flows are more affected by 'Re' than Newtonian ones. Also, for both Newtonian and drag reduction flows, 'Cp' is a maximum at 'D2/D1' $\approx 1.40$.

***Mean velocity profiles***

Samples of the upstream and downstream velocity profiles are shown in Fig.(9) . It is seen that appearance of drag reduction in the downstream pipe depends on the degree of drag reduction in the upstream one. Generally, the elastic sub layer thickness -i.e. the extent of drag reduction-in the downstream pipe is less than that in the upstream one. The limits of such behavior are determined by the onset conditions of drag reduction [11]. It is known that there is an onset wall shear stress, hence an onset Reynolds number 'Re $^*$', below which drag reduction doesn't occur. Thus, if ' $Re_2$' < 'Re $^*$' drag reduction is expected to disappear in the downstream pipe of the sudden-enlargement especially at low upstream drag reduction , i.e. low 'Df ', conitions. This behavior was recorded by the experimental observations due to Tachibana and Kita [18].

***Turbulence characteristics***

Figure (10) shows samples of the sudden enlargement effects on the turbulent kinetic energy (k) and its dissipation rate ($\varepsilon$ ) profiles under different values of damping factors 'Df' and Reynolds numbers. The upstream profiles are those predicted at the sudden enlargement entrance section while the downstream profiles are those at 50 diameters downstream from the entrance. It is seen that the sudden enlargement affects both (k) and ($\varepsilon$) in the same manner, for both Newtonian and drag reduction flows, where they decrease in the downstream direction. On the other hand, at the same distance from the wall, the value of either of 'k' or ' $\varepsilon$' under drag reduction conditions is less than that under Newtonian flow conditions and the difference-i.e. drag reduction effect- is higher near the wall .

***3- Experimental Work***

An experimental setup is designed to confirm the pressure distribution predictions. An additive technique, which helps in avoiding pump degradation effects on the test fluid, is adapted. In this technique, a master concentrated solution is mixed with the main pump flow. The mixture drag reduction effectiveness [22,23] is dependent on the master fluid polymer type, mixture concentration, pipe roughness and the additive technique. However, irrespective of polymer type and concentration, the fully developed flow friction factor data for the mixture- hence the damping factor 'Df' - is that required for theoretical predictions. Therefore, the main objective of the experimental setup is to measure the pressure distribution up-and-downstream a sudden enlargement in addition to the corresponding flow rate of the flowing mixture. In addition, primary tests of the pump degradation effects on polymer solutions indicated that drag reduction disappears as the concentrated solution flow is stopped.

Accordingly, the closed hydraulic circuit, shown in Fig.(11 ), is used in the experiments. It comprises a main tank (1), a circulating pump(2), concentrated polymer solution air pressurized tank(3) and the test section(4). Flow rates are measured using a collecting tank (5) and controlled using a control valve(8).Concentrated solution flow rates are measured using a level scale on the pressurized air tank(3). Wall static pressures are measured using an inclined, inverted , differential multi-tube manometer (6). The pressure of the concentrated solution tank is controlled using the pressure regulator (7) while the flow rate is controlled using a control valve (8) and is kept constant by observing the mercury manometer reading (9). The test section is a commercial steel sudden enlargement of diameter ratio (2:1) having its upstream pipe of '2.5' cm diameter and ' 150' cm length while the downstream one is ' 5' cm diameter and '60' cm length. Twelve static pressure tapes are distributed along the test section wall. The first five taps are distributed along the upstream pipe while the remaining seven taps are distributed along the downstream one. They have distances from the sudden enlargement section as shown in Table (3) below.

TABLE (3): Static Pressure Tap Distribution

| Tap No | 1 | 2 | 3 | 4 | 5 | 6 | 7 | 8 | 9 | 10 | 11 | 12 |
|---|---|---|---|---|---|---|---|---|---|---|---|---|
| Distance (cm) | 66.5 | 41.5 | 15 | 9 | 4 | 2.5 | 5.5 | 9.5 | 15 | 25 | 29.5 | 39.5 |

Tap water is used as the Newtonian fluid while dilute solutions of Polyethylene glycol (PEG) - of molecular weight $Mw=4*10^5$ - in tap water are used as the drag reducing fluids. Concentrated solutions are prepared and held for 24 hr before use in the pressurized tank. Fluid temperatures varied within $\pm$ 4 $C^o$ in all tests. The density and viscosity of the solutions are taken as those for pure water [11].

**Uncertainty Estimates**

Pressure distributions and flow rates are measured and the different dimensionless parameters such as the wall pressure '$Pw$', Reynolds number 'Re' and the friction factor 'f' are evaluated. An uncertainty analysis [24] resulted in the estimates shown in Table (4) below.

TABLE (4): Uncertainty Estimates

| Parameter | Range | Maximum % Uncertainty |
|---|---|---|
| discharge ($m^3/s$) | $3.6\text{-}6.9*10^{-4}$ | $\pm$ 5 |
| pressure drop(cm water) | 1.4-7.6 | $\pm$ 7 |
| dimensionless pressure drop '$Pw$' | 0.02-0.26 | $\pm$ 20 |
| Reynolds number 'Re' | 22465-42430 | $\pm$ 5 |
| friction factor 'f' | .0016-.0089 | $\pm$ 17 |

***Procedure***

Under steady state conditions, for certain openings of concentrated solution and main flow control valves, the manometer readings and flow rates are recorded simultaneously. Mixture concentration is calculated based on the measured flow rates of both of the concentrated solution and the dilute mixture. The corresponding upstream Reynolds number and friction factor, based on the readings of the upstream pressure taps (1) and (2) [see table(3)] , are calculated and allocated on Fig.(3). After allocating the experimental points, having the symbol (+) on the figure- the

corresponding damping factors 'Df ' required for the theoretical predictions are determined. Samples of the tested mixtures concentrations, the measured flow Reynolds numbers Re, friction factor 'f' and the corresponding 'Df' values are shown in Table(5) below.

TABLE (5) Test Fluid Data

| concentration (p.p.m.) | 0 | 1 | 5 | 18 | 34 | 42 |
|---|---|---|---|---|---|---|
| Re | 36960 | 22570 | 23870 | 38190 | 27280 | 42430 |
| $fx10^3$ | 6.65 | 8.1 | 5.45 | 4.41 | 3.75 | 3.74 |
| Df | 20 | 20 | 22 | 25 | 30 | 32 |

### *4. Comparison Between Theoretical and Experimental Results*

The present experimental pressure distribution results, of the (2:1) diameter ratio sudden enlargement are compared with theoretical predictions which are obtained for the above 'Re ' and ' Df' values. The comparison is shown in Figs (12) and(13). It is seen that there is a reasonable agreement between predicted and experimental results despite the uncertainty of the experimental data and the assumptions adapted in the theoretical analysis.

Early experimental pressure recovery coefficient ' G ' distributions for (1.76:1) and (2.6:1) diameter ratio sudden enlargement sections were presented by Tchibana and Kita [18]. They used two types of polymers but no details about the friction factor data were given. However, it has been established that the(mdr) condition is attained by all polymer solutions at a certain ultimate -polymer dependent- concentration [11]. Accordingly, their results under maximum concentrations of the used polymers are compared with the present predictions at Df=70 which corresponds to (mdr) condition. Fig.(14.a) shows the comparison for their 50 p.p.m. PEO solution while Fig.(14.c) shows the comparison for their 30 p.p.m. 'PAA' solution. Their results for Newtonian -i.e. water- flows are also compared with the present predictions at Df=20 and shown in Figs.(14.b) and (14.d) at two different Reynolds numbers. The figures indicate an acceptable agreement between the present theoretical predictions and their experimental results. Also, it is worthy to mention that the present predicted qualitative behaviors of the loss coefficient and the pressure recovery length, which are discussed in section 2.2 above, were early observed experimentally by Tachibana and Kita [18]. Thus, in addition to the decrease of the loss coefficient with drag reduction, they recorded that the pressure recovery distances ranged between $10 > Xp > 3$ for an upstream Reynolds number range $Re \cong 5000\text{-}12000$ and different concentrations of drag reducing polymers.

### *5. CONCLUSIONS*

Based on the above discussion, the following conclusions are drawn:

5.1) A 'k- ε' model for drag reducing fluids turbulent flow, under both favorite and adverse pressure gradients, has been developed . The model includes a damping factor which is determined from the fully developed pipe flow friction factor data.

5.2) Application of the model on flow through a sudden enlargement shows the following:

I) Drag reducing additives affect both the mean, and turbulence, flow characteristics which have the same trends as those of Newtonian fluids.

II) As drag reduction increases in the upstream pipe the maximum pressure recovery and its length increase while the loss coefficient ,turbulent kinetic energy and its dissipation rate decrease compared to the Newtonian values.

III) The down stream conditions of drag reduction are determined by the upstream ones and the onset criterion for a specific solution . In general, drag reduction decreases in the downstream pipe.

IV) For design purposes, plots of the predicted maximum pressure recovery are given. These plots indicate that a diameter ratio of (1.4:1) is an optimum design value for both Newtonian and drag reduction flows.

*REFERENCES*


1. Finnicum , D. S. and Hanratty, T. J., " Effect of favorable pressure gradients on turbulent boundary layers", J. AIChE, v.34, No.4, pp.529-540, (1988).
2. Jones, W. P. and Launder, B.E., " The prediction of laminarization with a two – equation model of turbulence", Int. J. Heat Mass Transfer, v.15,pp.301-314, (1972).
3. Lakshminaraya, B., "Turbulence modeling for complex shear flows", J.AIAA, v.24,No.12,pp.1900-1917, Dec.(1986).
4. Wolfgang, K., "Prediction methods for turbulent flows", Hemisphere Publishing Corp., (1980)
5. Bird, R.B., Stewart, W.E. and Lightfoot , E.N., " Transport phenomena", John Wiley& Sons inc.,N.Y, (1960).
6. Schlichting, H., "Boundary layer theory", N.Y., Mc Graw Hill, (1961).
7. Das, D. K. and White, F. M., " Integral skin friction prediction for turbulent separated flows" Trans. ASME , J. Fluids Engg., v.108, pp.476-482, (1986).
8. Khalifa, B.A., Embaby, M.H. and Mahfoz, F.M.," Developing laminar and turbulent flows in strongly curved rectangular ducts with high aspect ratio", Proceedings of the 7th Int. Conference of Mech. Power Eng. , v II, p. III/5,Fac. of Eng., Cairo Univ., Dec. 17-20, (1990).
9. Hattori, H. and Nagano, Y., " Calculation of turbulent flows with pressure gradients using a k- ε model", JSME Int. J., Series B, v.38, No.4, pp.518-524, (1995).
10. Lumley, J.L., "Drag reduction in turbulent flow by polymer additives", J. Polymer Sc., Macromolecular Reviews, v.7,pp.263-290, (1973).
11. Virk, P.S., "Drag reduction fundamentals", J. AIChE, v.21, No.4,, pp.625-656, (1975).
12. Poreh, M., Hassid, S., "Mean velocity and turbulent energy closures for flow with drag reduction", The Physics of Fluids, v.20, No.!0, pp.s193-s196, Oct. (1977).
13. Hassid, S. and Poreh, M., " A turbulent energy dissipation model for flows with drag reduction", Trans. ASME, J. Fluids Engg., v.100, pp. 107-111, (1978).
14. Rogeri, I. T., " Drag reduction in a model of shear flow turbulence", I&EC Fundamentals, v.7, 1, pp.32-38, (1968).
15. Durst, F. and Rastogi, A.K., "Calculations of turbulent boundary layer flows with drag reducing polymer additives", The Physics of Fluids, v.20,No.12, pp.1975-1985, Dec. (1977).
16. Idir, A. and Siamack, A.S. , " Numerical simulation of drag reducing turbulent flow in annular conduits", Trans.ASME, J. Fluids Engg., v.119,pp.838- 846, (1997).
17. Kato,H. and Shibanuma, H., "Diverging and converging flows of dilute polymer solutions( 1st Report , Pressure distribution and velocity profile) ",JSME ,v.23, No.181, pp.1140-1147, (1980).
18. Tachibana, M. and Kita, M., "On the flow in a circular section tube and the loss due to a sudden enlargement (Effect of drag reducing additives) ", JSME, v21, No.159, pp.1341-1348, (1978).
19. Lee, B.K., Cho, N. H. and Choi, Y. D. , " Analysis of periodically fully developed turbulent flow and heat transfer by k- ε equation model in artificially roughened

annulus", Int. J. Heat Mass Transfer,v.31,No.9, pp.1797-1806, (1988).
20. Patankar, S.V., "Numerical heat transfer and fluid flow", Mc Graw Hill, (1980).
21. Virk, P.S., " Drag reduction in rough pipes", J. Fluid Mech., v.45,part 2, pp.225-246,(1971).
22. Klaus, W. H. and Albert, G, "Heterogeneous drag reduction concepts and consequences", Trans. ASME, J. Fluids Eng., v.120, pp.818-823, Dec.(1998).
23. Walker, D.T., Tiederman, W.G. and Luchik , T.S., " Optimization of the injection process for drag-reducing additives ", Experiments in Fluids , v.4, pp.114- 120, (1986).
24. Moffat, R. J., "Contributions to the theory of single –sample uncertainty analysis" , Trans. ASME, J. Fluids Engg.,v.104,pp.250-260, (1982).

## *NOMENCLATURE*

| | |
|---|---|
| $A^+$ | dimensionless function in the turbulence model ; |
| AR | area ratio of sudden enlargement ; |
| $B_1$ ,$B_2$ | constants in the turbulence model ; |
| $C_1$ ,$C_2$,$C_\mu$ | constants in the turbulence model ; |
| D' | pipe diameter (m) ; |
| Cp | dimensionless maximum pressure recovery ; |
| Df | damping factor in the turbulence model ; |
| f | friction factor $=\tau'_w/(.5\rho U'^2)$ ; |
| $f_\varepsilon, f_\mu$ | functions in the turbulence model ; |
| G | rate of pressure recovery ; |
| k' , k | turbulent kinetic energy ( $m^2/s^2$ ), dimensionless = k' / U'$^2$ ; |
| p' , p | pressure (pa), dimensionless $=(p'-p'_1)/\rho U'^2$ ; |
| $P_k$ | production of turbulent kinetic energy ; |
| $P^+$ | pressure gradient function $=\nu'(dp'/dx')/\rho u'^3_\tau$ ; |
| r' ,r | radial coordinate(m), dimensionless =r'/ $D'$ ; |
| R' , R | pipe radius (m), dimensionless = R' / $D'$ ; |
| Re, $R_t$ | Reynolds number $=D'U'/\nu'$, turbulence Reynolds number $=k^2/\nu\varepsilon$ ; |
| $S_\phi$ | dimensionless source term ; |
| u', u | axial velocity component(m/s), dimensionless =u'/ U' ; |
| $u_\tau$' ,$u_\tau$ | wall shear velocity = $\sqrt{\tau'_w/\rho}$ (m/s), dimensionless =u'$_\tau$/ U' ; |
| U' | average velocity (m/s) ; |
| u+ | dimensionless velocity = u' / u'$_\tau$ ; |
| v', v | radial velocity component (m/s), dimensionless =v'/ U' ; |
| x', x ,X | axial coordinate (m), dimensionless = x'/D', dimensionless axial domain length ; |
| Xp | dimensionless pressure recovery length ; |
| y, y+ | distance from wall (m), dimensionless =y' u'$_\tau$/ $\nu'$ ; |

## *GREEK SYMBOLS*

| | |
|---|---|
| $\Gamma_\phi$ | property diffusion coefficient ; |
| $\varepsilon'$, $\varepsilon$ | turbulent kinetic energy dissipation rate(m$^3$/Kg.s), dimensionless = $\varepsilon'\ \rho$ D'/ U' ; |

| | |
|---|---|
| $\mu'_l, \mu_l$ | dynamic viscosity (Pa.s),dimensionless=1/Re ; |
| $\mu_e$, $\mu_t$ | dimensionless effective viscosity, turbulent viscosity ; |
| $\nu'$, $\nu$ | kinematic viscosity ($m^2/s$), dimensionless=1/Re ; |
| $\xi$ | sudden enlargement loss coefficient ; |
| $\rho$ | density ($Kg/m^3$) ; |
| $\sigma_k, \sigma_\varepsilon$ | constants in the turbulence model ; |
| $\tau_w'$, $\tau_w$ | wall shear stress (Pa), dimensionless $= \tau_w' / (\rho U'^2)$ ; |
| $\phi$ | transport property variable . |

***Subscripts***

| | |
|---|---|
| 1 | evaluated at the end of the upstream pipe ; |
| 2 | evaluated for the downstream pipe ; |
| max | maximum value of a parameter ; |
| p | evaluated near the wall ; |
| w | evaluated at the wall ; |
| wr | evaluated at the wall in radial direction . |

***Superscripts***

| | |
|---|---|
| ' | dimensional quantity |

***Abbreviations***

| | |
|---|---|
| APG | adverse pressure gradient ; |
| FPG | favorite pressure gradient ; |
| mdr | maximum drag reduction . |

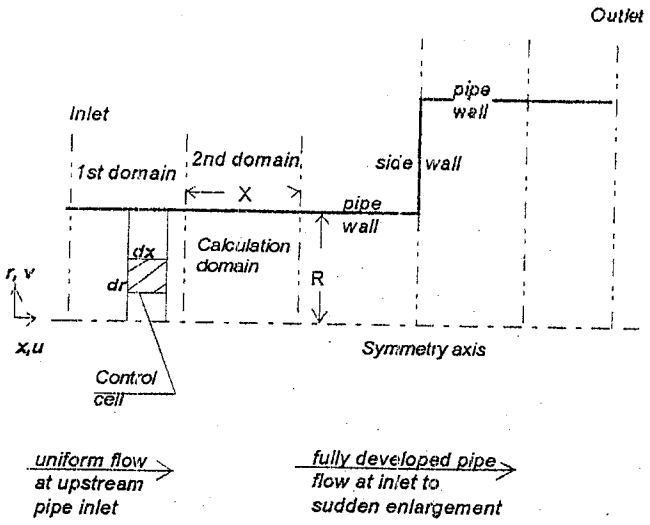


FIG.( 1 ) Geometry and calculation domains.

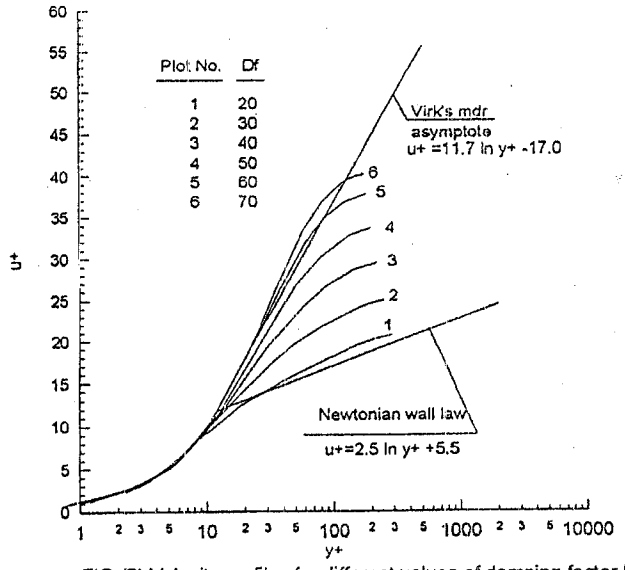


FIG.(2) Velocity profiles for different values of damping factor Df.

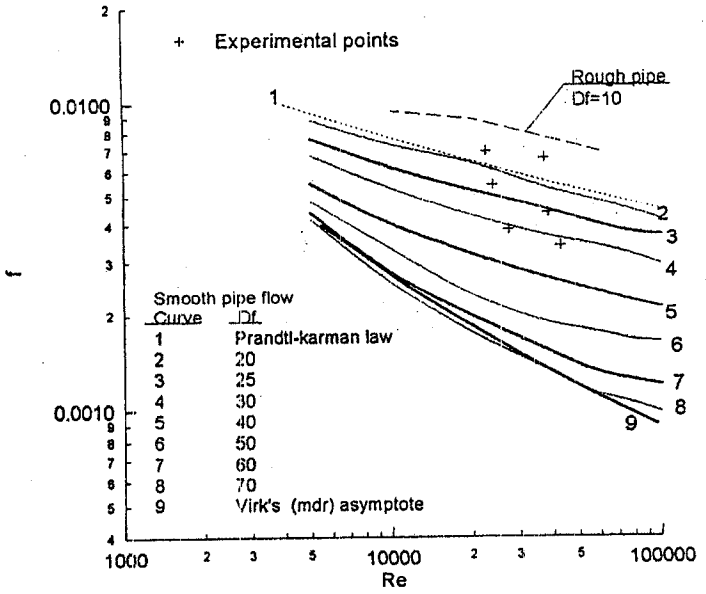


FIG.( 3 ) Predicted fully developed pipe turbulent flow ' f - Re' relationships for different values of damping factor Df.

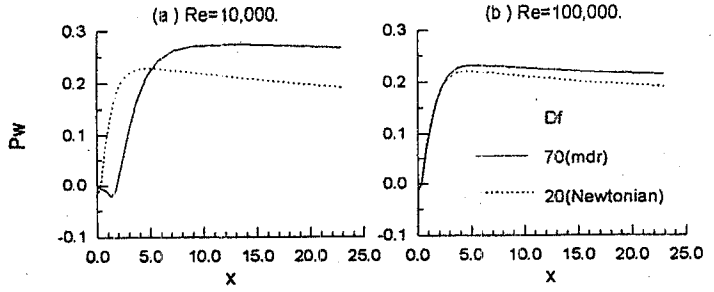


FIG.(4)Wall static pressure 'Pw' variation along a sudden enlargement.

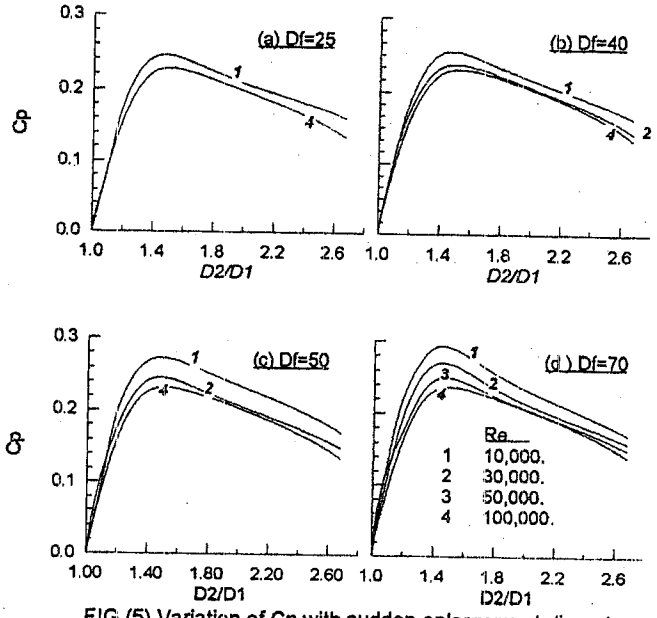


FIG.(5) Variation of Cp with sudden enlargement diameter ratio,(effect of Re).

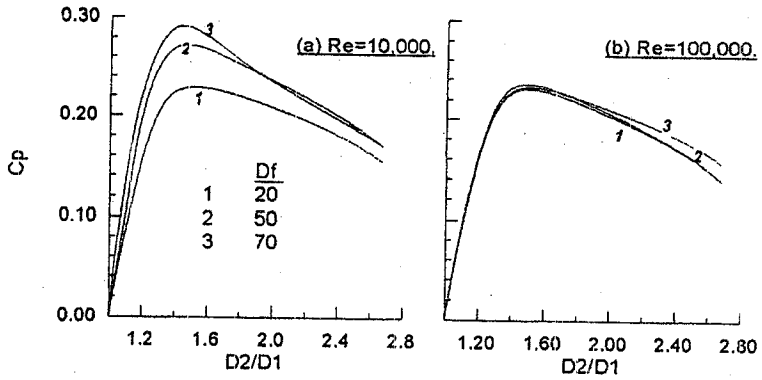


FIG.(6) Variation of pressure coefficient Cp with diameter ratio, (effect of drag reduction damping factor Df).

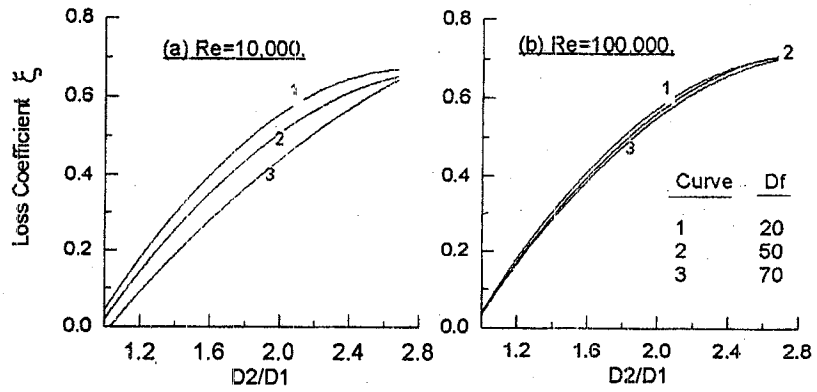


FIG.(7) Variation of loss coefficient with diameter ratio ( effect of drag reduction damping factor Df ).

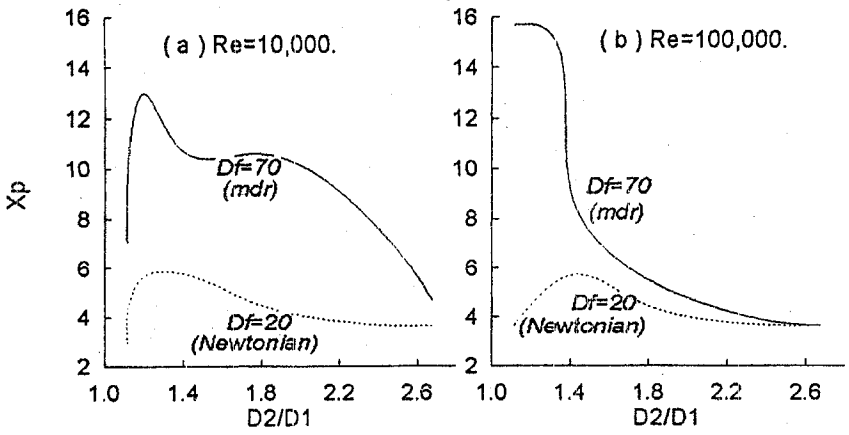


FIG.(8)Variation of pressure recovery length 'Xp' with diameter ratio (D2/D1).

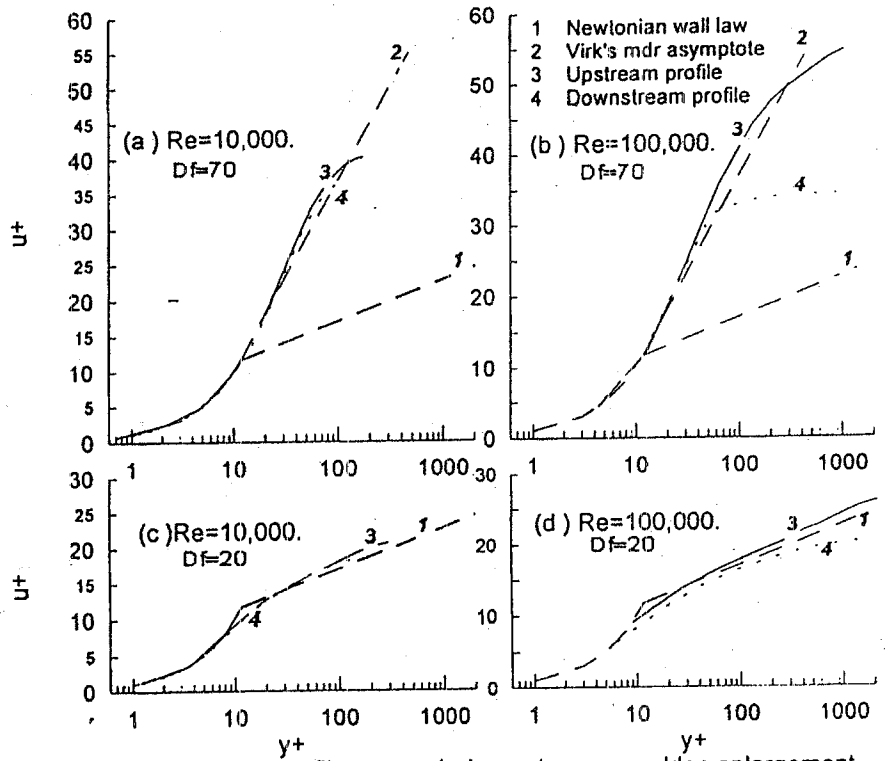


FIG.(9 ).Velocity profiles up-and -down stream a sudden enlargement, ( D2/D1=1.75).

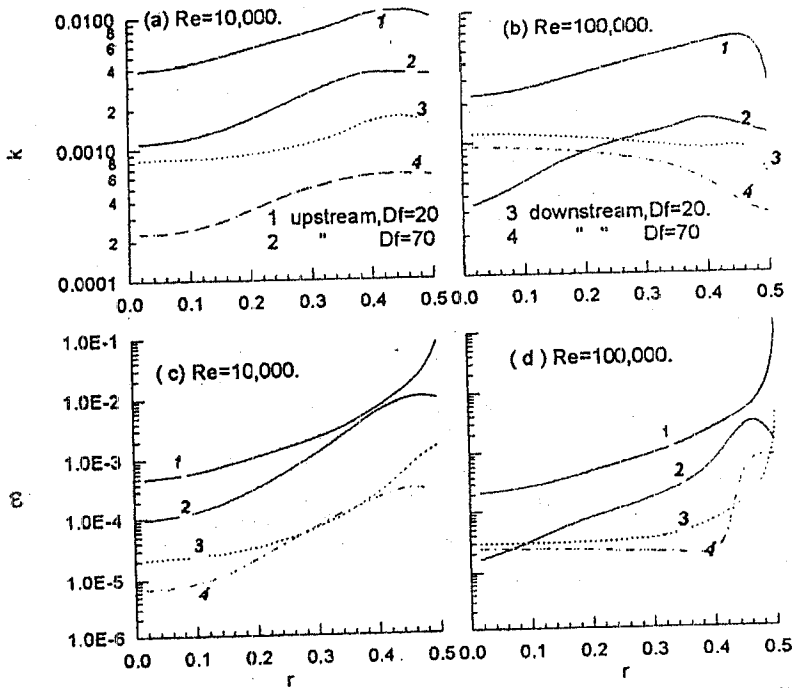


FIG.(10)Turbulent kinetic energy 'k' and its dissipation 'ε' distributions up and downstream of a sudden enlargement(D2/D1=1.75) .

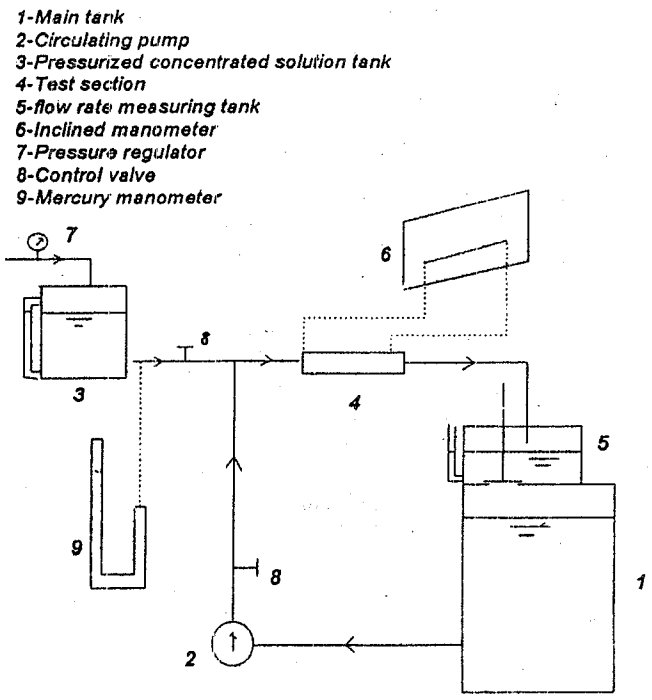


FIG.(11 ) Experimental test rig.

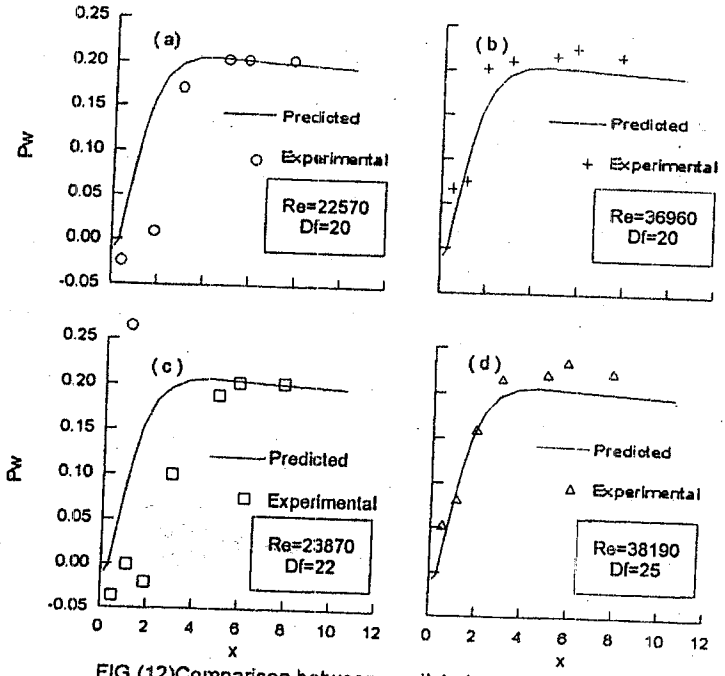


FIG.(12)Comparison between predicted and present experimental pressure distributions along a sudden enlargement ( D2/D1=2).

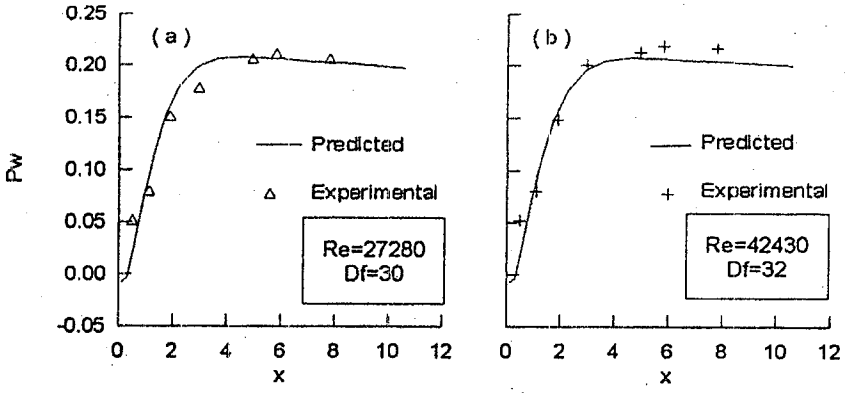


FIG.(13) Comparison between predicted and experimental pressure distributions along a sudden enlargement ( D2/D1=2).

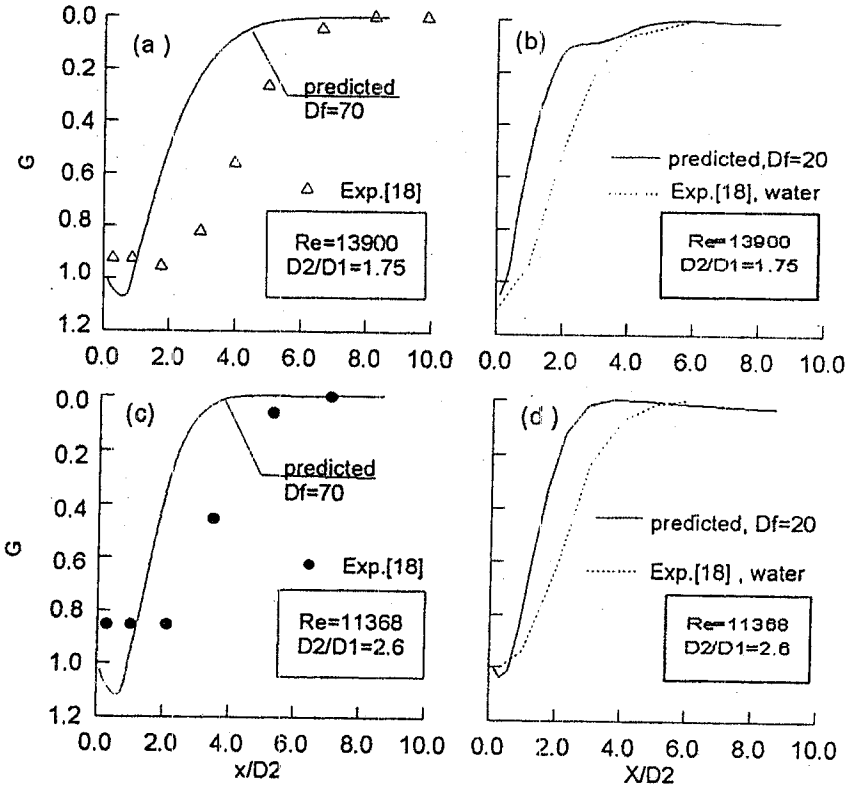


FIG. (14 ) Comparison between theoretical and early[18] experimental rates of pressure recovery .

# ملخص البحث

## FLOW OF DRAG REDUCING FLUIDS THROUGH A SUDDEN ENLARGEMENT

*M.H.Embaby and M.A. El-Kadi*
*Mechanical Power Engineering Department, Faculty of Engineering, Minufiya University, Egypt.*

## سريان الموائع المقللة للاحتكاك خلال مقطع ذى اتساع مفاجئ

أجريت دراسة نظرية و معملية لسريان الموا ئع المقللة للاحتكاك خلال مقطع دائرى ذو اتساع مفاجئ.

فى الدراسة النظرية , تم تطوير نموذج اضطراب – استخدم فى أ بحاث سابقة لاستنتاج خصائص السريان الاضطرابى للموائع النيوتونية تحت تأثير تدرج ضغطى معاكس – تم تطوير هذا النموذج حتى يمكن استنتاج خصائص السريان الاضطرابى للموائع المقللة للاحتكاك . و باستخدام هذا النموذج المطور امكن وبشكل جيد استنتاج خصائص السريان الاضطرابى لهذه الموائع خلال الأنابيب مستديرة المقطع ( أى تحت تأثير تدرج ضغطى مواكب) وأيضا السريان خلال الاتساع المفاجئ ( أى تحت تاثير تدرج ضغطى معاكس) . وقد تم شرح ومناقشة هذه الخصائص والتعليق عليها.

وقد تم انشاء جهاز معملى لدراسة خصائص توزيع الضغط للسريان خلال مقطع اختبار نسبة قطريه (2:1) .واستخدمت محاليل مخففة –من مادة البولى ايثيلين جليكول فى الماء بتركيزات مختلفه – كموائع مقللة للاحتكاك. وأجريت مقارنة النتائج النظرية بالنتائج العملية الحالية و بعض النتائج العملية من أ بحاث سابقة وأظهرت المقارنه توافقا مقبولا.

وخلصت الدراسة الى ان نموذج الاضطراب المطور – الذى تم التوصل اليه فى هذا البحث – يمكن استخدامه لاستنتاج خصائص السريان الاضطرابى للموائع المقللة للاحتكاك تحت تاثير اى من التدرج الضغطى المواكب او التدرج الضغطى المعاكس.